

# Relative Wulst volume is correlated with orbit orientation and binocular visual field in birds

Andrew N. Iwaniuk  Christopher P. Heesy   
Margaret I. Hall  Douglas R. W. Wylie

Received: 15 March 2007 / Revised: 20 November 2007 / Accepted: 24 November 2007 / Published online: 11 December 2007  
Springer-Verlag 2007

**Abstract** In mammals, species with more frontally oriented orbits have broader binocular visual fields and relatively larger visual regions in the brain. Here, we test whether a similar pattern of correlated evolution is present in birds. Using both conventional statistics and modern comparative methods, we tested whether the relative size of the Wulst and optic tectum (TeO) were significantly correlated with orbit orientation, binocular visual field width and eye size in birds using a large, multi-species data set. In addition, we tested whether relative Wulst and TeO volumes were correlated with axial length of the eye. The relative size of the Wulst was significantly correlated with orbit orientation and the width of the binocular field such that species with more frontal orbits and broader binocular fields have relatively large Wulst volumes. Relative TeO volume, however, was not significantly correlated with either variable. In addition, both relative Wulst and TeO volume were weakly correlated with relative axial length of the eye, but these were not corroborated by independent contrasts. Overall, our results indicate that relative Wulst

**Keywords** Evolution Wulst Optic tectum Binocularly Eye size

**Abbreviations**  
GLd Nucleus geniculatus lateralis, pars dorsalis  
GLv Nucleus geniculatus lateralis, pars ventralis  
HA Apical hyperpallium  
HD Densocellular part of the hyperpallium  
HI Interstitial part of the hyperpallium  
IHA Intercalated part of the hyperpallium  
LGN Lateral geniculate nucleus  
S1 Primary somatosensory cortex  
TeO Optic tectum  
V1 Primary visual cortex  
W Wulst

A. N. Iwaniuk (& ) · D. R. W. Wylie  
Department of Psychology, University of Alberta,  
Edmonton, AB T6G 2E9, Canada  
e-mail: brainsize@yahoo.ca

C. P. Heesy  
Department of Anatomy, Midwestern University,  
Glendale, AZ 85308, USA

M. I. Hall  
Department of Biomedical Sciences, Midwestern University,  
Glendale, AZ 85308, USA

D. R. W. Wylie  
Centre for Neuroscience, University of Alberta,  
Edmonton, AB T6G 2E9, Canada

## Introduction

Orbit orientation varies tremendously among birds from the laterally placed eyes of the woodcock (*Scolopax rusticola*; Martin 1994) to the more frontally oriented eyes of owls. The orientation of the orbits has significant implications for the shape and size of the visual field. More laterally oriented orbits result in a broad visual field, but at the cost of a narrower binocular visual field (e.g., Martin 1994). More frontally oriented orbits, however, result in a larger binocular visual field, but at the cost of a large posterior blind field (e.g., Martin 1984). In mammals, species with frontally oriented orbits tend to have broader

binocular fields (Heesy 2004) and both frontal eyes and primary somatosensory (S1) and motor (M1) cortices of broad binocular fields are correlated with the relative size of mammals (Medina and Reiner 2000; Reiner et al. 2005). Because it is difficult to separate the somatomotor from visual regions in the brain. For example, the relative sizes of the lateral geniculate nucleus (LGN), primary visual cortex (V1) and the entire neocortex are all positively correlated with more frontally oriented and convergent orbits in primates (Bartlett 2004). That is, the sizes of these visual regions are larger in those species with more frontally oriented and convergent eyes. Whether orientation evolution in mammals is similar to that of birds, we know that this is not the case. In mammals, whereas in birds, we know that this is not the case. In mammals, however, remained unexplored.

Based upon physiological, developmental and hodological evidence, the homolog of the mammalian V1 in birds is the visual Wulst (Karten et al. 1973; Pettigrew 1979; Shimizu and Karten 1993; Medina and Reiner 2000; Husband and Shimizu 2001; Reiner et al. 2005). In a similar fashion to V1, the Wulst is retinotopically organized (Pettigrew 1978, 1979) and electrophysiological studies of owls and raptors have shown that the majority of cells in the Wulst have receptive fields in the area of binocular overlap in the visual field and many are binocular with disparity sensitivity (Pettigrew and Konishi 1976; Pettigrew 1978, 1979). Given the marked similarity between V1 and Wulst and the likely role of the Wulst in mediating binocularity in more frontally eyed birds, it would seem reasonable to predict that relative Wulst size might be correlated with both orbit orientation and size of the binocular visual field. There are, however, several caveats that could affect this relationship between the Wulst and the peripheral visual system.

Although a link between the Wulst and binocularity has been demonstrated in more frontally eyed species, the data for more laterally eyed birds is inconclusive. For example, binocular cells with frontal receptive fields are present in the domestic chick (*Gallus domesticus*) (Wilson 1980), but similar cells have not been discovered in pigeons (*Columba livia*) (Miceli et al. 1979, despite the fact that pigeons are capable of stereopsis (McFadden and Wilke 1986). Binocular cells are present in other structures in pigeons, such as the nucleus of the basal optic root (nBOR) (Wylie and Frost 1990), but these have receptive fields up to 180° and are therefore not associated with stereopsis. Thus, the association between the Wulst and binocularity and stereopsis may not be true of all birds.

In addition to the uncertainty regarding the role of the Wulst in binocularity and stereopsis, it is important to recognize that unlike V1, the Wulst is not an exclusively visual structure. The Wulst also receives substantial somatosensory and kinesthetic input (Funks 1989; Deng and Wang 1993; Wild 1997; Wild and Williams 2000; Manger et al. 2002). As a whole, the Wulst can therefore be considered homologous to not only V1, but also the

Convergence is defined as the dihedral angle (an angle between two planes) between the orbital margin plane and the midsagittal plane (e.g., Cartmill 1970) (illustrated in Fig. 1). This dihedral angle is formed by the intersection of the orbital and sagittal planes rostrally (Fig. 1). A low value of convergence indicates a small deviation of the orbital plane away from the sagittal plane, whereas a higher value of convergence indicates the orbital plane deviates comparatively more from the sagittal plane and faces more rostrally. Three points define the planes. In order to be comparable with the previous studies, the following points were analogized from mammalian skull anatomy. The sagittal plane is defined by (1) the anterior-most point of the beak (comparable to mammalian prosthion); (2) that point where the internasal suture meets the inter-premaxillary suture (mammalian nasion); and (3) the posterior-most projection on the skull, at the superior-most portion of the occipital complex (comparable to mammalian inion). The orbital plane is also defined by three points: (1) orbitale inferius defined in mammals as that point on the orbital margin closest to the alveolar margin, and in birds as the mid-point on the quadratojugal bar; (2) orbitale superius defined in both mammals and birds as that point on the orbital margin that is directly opposite and furthest from orbitale inferius; and (3) orbitale anterius defined in mammals as the point on the orbital margin most distant from the inion. In the avian skull, we defined orbitale anterius as the central point of the lacrimal bone, which corresponds to the point furthest from the avian equivalent of the mammalian inion, the occipital complex. However, in many birds, including most of the birds in this sample, the lacrimal bone is highly pneumatized at that point to create a lacrimal bulge, which may act as an anchor for the anterior portion of the sclerotic ring within the orbit. Therefore orbitale anterius was measured at the superior-most point of the bulging area. These three-dimensional coordinate data were collected for the six landmark points on the skull with a Microscribe-3DX coordinate data stylus (Immersion Corp., San Jose, CA, USA). Each specimen was mounted on an elevated clay base so that all coordinate data could be collected in a single series (Lockwood et al. 2002). Each specimen sits within its own three-dimensional coordinate data space with this arrangement. The orbit convergence was calculated from these coordinate data following standard trigonometric function for dihedral angle computation (e.g., Beyer 1979). A macro for this calculation is available in Heesy 2003. The dihedral angle is the angle  $\alpha$  between the planes, which are defined as:

$$A_1x + B_1y + C_1z + D_1 = 0 \text{ and} \\ A_2x + B_2y + C_2z + D_2 = 0,$$

which have normal (i.e., perpendicular) vectors,

where the sagittal plane is defined as (referring to landmarks in Fig. 1)  $n_1 = A_1x + B_1y + C_1z + D_1$  and  $n_2 = A_2x + B_2y + C_2z + D_2$  and the orbital plane is defined as (referring to landmarks in Fig. 1),  $n_1 = A_1x + B_1y + C_1z + D_1$  and  $n_2 = A_2x + B_2y + C_2z + D_2$ . The dot product of the normals is,  $\cos \alpha = \frac{n_1 \cdot n_2}{|n_1| |n_2|}$ .  $\cos \alpha = \frac{A_1A_2 + B_1B_2 + C_1C_2 + D_1D_2}{\sqrt{A_1^2 + B_1^2 + C_1^2 + D_1^2} \sqrt{A_2^2 + B_2^2 + C_2^2 + D_2^2}}$  or (referring to landmarks in Fig. 1)  $\cos \alpha = \frac{OA \cdot OS + N \cdot OA + P \cdot OI}{\sqrt{OA^2 + OS^2} \sqrt{N^2 + P^2 + OI^2}}$ .

Arccosine transformation produces the angle or the angle of convergence for a single orbit. Alternatively, this angle can be thought of as the inverse of the angle of divergence, but convergence is already in use in the mammalian literature (e.g., Barton 2004; Heesy 2003), so for consistency, we have used convergence. The angles were then multiplied by 2 to yield the total (or bilateral) convergence of both orbits. The total orbit convergence could then be compared to the width of the binocular visual field, which is the amount of overlap between each monocular visual field.

The measurements were taken using the same landmarks for all species, with two exceptions, the Grey Potoo (*Nyctibius griseus*) and the Pauraque (*Nyctidromus albigularis*). In these two species, the quadratojugal bars are extremely bowed (Fig. 2), which resulted in large orbital convergence values (>100) compared to other caprimulgidiform birds and all other birds measured (Table 1). Furthermore, they were significant outliers (i.e., 3 standard deviations from the mean) in all bivariate and multivariate analyzes. Therefore, for these two species, we drew a hypothetical straight line between the rostral and caudal ends of the quadratojugal bars and used the midpoint along this line as the  $OIO$  landmark (Fig. 2). The convergence values using this landmark were still large, but were more in line with other caprimulgidiforms (Table 1) and did not prove to be significant outliers. It should, however, be noted that our conclusions did not differ if these two species were excluded from our analyzes or if we used the extreme values, but the amount of variation explained did decrease.

Table 1 A list of the species surveyed, sample sizes (orbital/neural measurements), orbital convergence (in degrees), binocular visual field (bracketed), axial length, brain, Te, W, TeO tectum (TeO) volumes (all in mm<sup>3</sup>)

Order	Species	n	Orbital convergence	Binocular visual field	Axial length	Brain	Te	W	TeO
Anseriformes	<i>Anas platyrhynchos</i>	3/8	24.54	8	13.50	5,738	3720.47	572.23	251.48
	<i>Dendrocygna eytoni</i>	2/1	58.07		12.20	4,850	3185.84	499.07	163.65
Apodiformes	<i>Chaetura pelagica</i>	2/1	44.36			343	159.92	16.61	30.47
	<i>Aegothales insignis</i>	1/1	50.87		14.05	1,540	1108.00	363.63	73.64
Caprimulgiformes	<i>Caprimulgus</i> sp.	2/1	71.64			734	342.75	51.62	58.81
	<i>Nyctibius griseus</i>	1/1	89.6		20.40	1,980	1004.67	176.67	125.58
Charadriiformes	<i>Nyctidromus albigollis</i>	3/1	62.7	25	13.40	910	414.83	66.03	36.95
	<i>Podargus strigoides</i>	2/3	62.64	50	24.57	5,311	3826.81	1226.89	290.88
	<i>Steatornis caripensis</i>	2/1	52.43	38	15.46	3,900	2887.70	749.53	104.7
	<i>Calidris minutilla</i>	1/1	36.03		6.13	472	255.50	12.66	43.34
	<i>Charadrius vociferus</i>	1/1	14.21		10.60	1,073	523.69	19.74	130.65
	<i>Limnodromus griseus</i>	1/2	34.26		8.80	1,124	725.11	33.92	51.12
	<i>Sterna hiruendo</i>	3/1	28.16			1,593	808.53	57.09	121.49
	<i>Vanellus miles</i>	2/1	13.45		14.00	2,686	1573.48	127.85	205.47
	<i>Ardea cinerea</i>	3/1	14.70		18.70	8,446	5028.04	520.41	697.78
	<i>Bubulcus ibis</i>	3/1	26.06	22		4,025	1939.45	220.7	211.02
Ciconiiformes	<i>Egretta thula</i>	2/1	19.81	15		3,740	1973.5	196.41	443.74
	<i>Nycticorax caledonicus</i>	3/1	32.59	22	17.80	3,360	1921.54	224.17	268.95
	<i>Columba livia</i>	3/8	49.59	22	9.40	2,093	1014.72	187.43	198.29
Coraciiformes	<i>Dacelo novaeguineae</i>	3/4	48.10	32		3,515	2097.42	176.3	333.9
	<i>Falco cenchroides</i>	1/1	41.10		15.3	3,211	1847.78	252.55	213.73
Falconiformes	<i>Falco peregrinus</i>	2/1	74.52		20.5	6,187	3426.94	529	338.21
	<i>Alectoris chukar</i>	2/1	46.92		13.5	2,500	1406.39	164.61	213.36
Galliformes	<i>Chrysolophus pictus</i>	3/1	27.81			3,369	1726.01	175.12	316.06
	<i>Colinus virginianus</i>	3/1	38.33		9.9	1,091	569.85	69.18	112.3
Passeriformes	<i>Coturnix coturnix</i>	2/	50.20		8.3	811	419.09	71.25	87.47
	<i>Gallus domesticus</i>	3/1	38.56		15.0	2,993	1242.46	132.34	279.55
	<i>Meleagris gallopavo</i>	2/	14.06		19.5	7,990	3764.53	469.04	771.14
	<i>Numida meleagris</i>	3/1	43.64		14.3	3,951	2223.28	228.52	328.46
	<i>Ortalis canicollis</i>	1/1	24.18			3,374	1829.65	203.83	271.27
	<i>Phasianus colchicus</i>	3/1	35.69		15.05	1,865	1999.35	322.69	304.9
	<i>Entomyzon cyanotis</i>	1/1	25.59		10.7	2,227	1580.07	129.88	97.04
	<i>Garrulus glandarius</i>	1/3	41.04		14.05	3,943	2596.73	448.99	248.9
	<i>Passer domesticus</i>	3/6	34.35		6.15	989	637.56	117.09	62.69

Table 1 continued

Order	Species	n	Orbital convergence	Binocular visual field	Axial length	Brain	Te	W	TeO
Procellariiformes	<i>Puffinus tenuirostris</i>	1/1	34.96	14	12.8	4,658	2334.24	442.32	235.01
	<i>Agapornis personata</i>	3/1	15.15			2,786	2069.65	204.54	82.57
Psittaciformes	<i>Agapornis roseicollis</i>	3/1	10.34			2,008	1454.88	194.32	79.74
	<i>Alisterus scapularis</i>	3/3	14.12		12.4	4,779	3274.72	506.55	201.21
	<i>Amazona aestiva</i>	2/1	15.94			7,903	5672.01	759.2	272.5
	<i>Aratinga acuticaudata</i>	2/1	12.71			5,222	4325.91	240.73	114.88
	<i>Cacatua roseicapilla</i>	3/1	31.07		12.1	6,653	4908.67	676.33	203.44
	<i>Calyptorhynchus funereus</i>	2/1	7.84		16.6	16,078	12823.60	2036.7	307.5
	<i>Eclactus rotatus</i>	2/2	9.73		13.8	6,700	4780.89	701.68	221.1
	<i>Glossopsitta concinna</i>	3/3	10.75		8.1	3,150	2280.26	368.43	111.79
	<i>Meiopsittacus undulatus</i>	1/1	56.45		6.9	1,220	825.12	84.35	59.64
	<i>Myiopsitta monachus</i>	1/	30.33		8.7	3,697	2733.13	253.61	156.38
	<i>Nymphicus hollandicus</i>	3/2	19.55		7.54	2,339	1676.78	247.88	81.29
	<i>Pionus menstruus</i>	1/1	24.97		10.57	5,473	3851.82	408.63	257.95
	<i>Platycercus elegans</i>	/3	32.82			3,822	2687.55	348.05	158.3
	<i>Polytelis swainsonii</i>	2/2	38.29			3,149	2153.13	288.77	170
	<i>Psephotus haematonotus</i>	2/2	29.19		8.4	1,914	1402.55	174.56	73.47
	<i>Psittacula krameri</i>	1/1	24.03		9.8	4,239	3269.62	565.67	120.45
<i>Pyrrhura molinae</i>	2/1	5.59		8.5	4,656	3123.51	497.19	232.93	
<i>Trichoglossus haematodus</i>	1/2	36.75		9.95	3,726	2726.62	409.77	125.6	
Rheiformes	<i>Rhea americana</i>	1/1	66.86		32.48	19,228	10281.3	2295.13	1286.6
Sphenisciformes	<i>Spheniscus magellanicus</i>	3/1	49.86	28		16757	10890.20	2362.55	672.29
	<i>Aegolius acadicus</i>	0/1		50	15.65	2,857	2009.90	743.75	64.49
Strigiformes	<i>Athene cucularia</i>	2/1	66.78			5,878	4813.8	1707.67	148.71
	<i>Ninox boobook</i>	2/2	75.26		22.3	5,626	3920.44	1503.68	148.15
	<i>Tyto alba</i>	3/1	81.44	44	17.8	6,149	4108.53	1605.41	136.51

Sources for the axial length, binocular visual field and brain data included the following: Riffers (Ebinger and Ebner (1984), Martin and Young (1984), McFadden and Wild (1989), Boire (1989), Martin and de L. Brooke (1991), Rehkemper et al. (1991), Alma and Bee de Speront (1992), Katzir and Martin (1994, 1999), Carezzano and Bee de Speront (1995), Ebinger (1995), Fernandez et al. (1997), Martin et al. (2004), Iwaniuk and Wylie (2004), Hall and Ross (2007) and Martin (1986)

<sup>a</sup> Data is listed from a congener (see materials and methods)

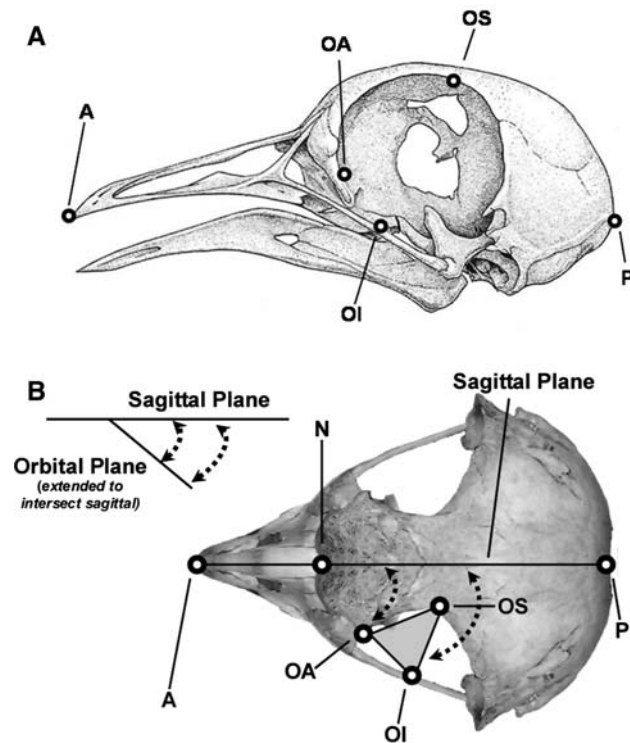


Fig. 1 Morphometric points used to define orbital and sagittal planes are illustrated on Pigeon (*Columba livia*) in lateral view (a) and Snowy Owl (*Nyctea scandiaca*) in dorsal view (b). The sagittal plane is defined by points A, N, and P. The orbital plane is defined by the points OS, OI, OA. Convergence is the dihedral angle formed by the intersection of the orbital and sagittal planes rostrally. (Abbreviations (see text for full definitions): A anterior-most point on the beak, N point of union between the internasal and intermaxillary sutures, P posterior-most point on the skull, OS orbitale superius, OI orbitale inferius, OA orbital anterius. (Illustration of *Columba livia* redrawn and modified from Proctor and Lynd 1993)

### Binocular visual field

Data on the breadth of the area of binocular visual field was taken from the literature for 13 species (Table 1). In order to expand the number of species included in our analyses, we included data for congeners of the following species-pairs: *Egretta garzetta* (Katzir and Martin 1994) for *Egretta thula*; *Nycticorax nycticorax* (Katzir and Martin 1998) for *Nycticorax caledonicus*; *Puffinus puffinus* (Martin and de L. Brooke 1991) for *Puffinus tenuirostris* and *Spheniscus humboldti* (Martin and Young 1984) for *Spheniscus magellanicus*. Because these may not truly reflect the visual fields of congeners, we performed our analyses both including and excluding these four species.

### Brain measurements

Forty-eight specimens representing 31 species were collected from wildlife sanctuaries and veterinary clinics

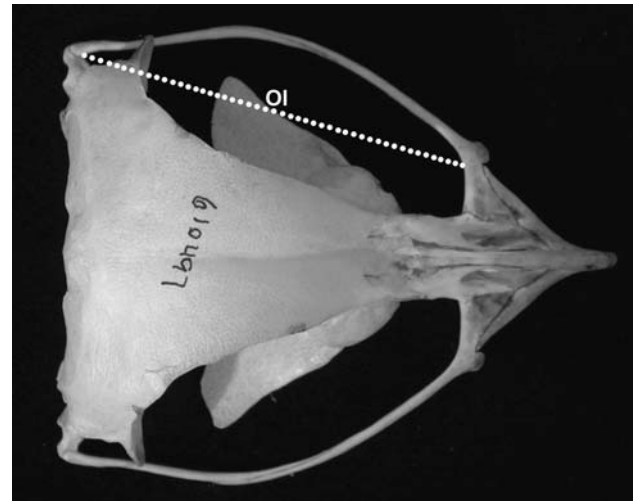


Fig. 2 A dorsal view of a Grey Potoo (*Nyctibius griseus*) skull (USNM 610497). The dotted white line indicates the line drawn between the rostral and caudal ends of the quadratojugal bars used to calculate orbital convergence in this species and the Pauraque. Note that the quadratojugal bars are extremely bowed laterally compared to the Snowy Owl (*Nyctea scandiaca*) shown in Fig. 1

and sent to us from other researchers. The heads of these specimens were immersion fixed in formaldehyde for one to several weeks, the brains extracted, weighed to the nearest milligram and stored in formaldehyde until processing. In addition, several specimens were loaned to use from the National Museum of Natural History (Washington, DC, USA) and the Bishop Museum (Honolulu, HI, USA) (see Iwaniuk and Wylie 2006). The brains of the museum specimens, which were all stored in 70% ethanol for up to 45 years, were extracted and placed into buffered 4% paraformaldehyde.

For all specimens, tissue processing was identical. The fixed brains were placed into 30% sucrose in 0.1 M phosphate buffered saline (pH = 7.4) until they sank. The brains were then embedded in gelatin and serially sectioned in the transverse plane on a freezing stage microtome at 40  $\mu$ m. The sections were collected in 0.1 M phosphate-buffered saline, mounted onto gelatinized slides, stained for Nissl substance with thionin and coverslipped with Permount. Digital photographs were taken throughout the brain for every second section, and the volumes of the telencephalon, Wulst and TeO were measured with the public domain NIH Image program (<http://rsb.info.nih.gov/nih-image/>).

The apical hyperpallium (HA), interstitial part of the hyperpallium (HI), intercalated part of the apical hyperpallium (IHA), and densocellular part of the hyperpallium (HD) were all included in the Wulst measurements (Table 1) as in Iwaniuk and Wylie (2006). It was not possible to calculate the volumetric fractions of each of these Wulst subdivisions because they could not be

reliably delineated throughout the extent of the Wulst for possible that relative Wulst and TeO volumes are correlated in many specimens and this information was largely unavailable for other species in the literature. The borders were delineated by: the vallicula laterally, the superior frontal lamina ventrally and the ventricle medially. We defined the caudal pole as the point at which the vallicula could no longer be recognized and the hippocampal information was present.

We also measured the volume of the optic tectum and focal length (TeO) for two reasons. First, there is the possibility that the expansion of one part of the visual system is correlated with size changes in other parts of the visual system. Such patterns of correlated evolution among brain structures are, in fact, common in mammals. Eye measurements followed that are outlined in Ritland et al. (2004). Second, based on several pieces of evidence, Gunturkun and Hahmann (1999) suggested that the optic tectum (TeO), and not the Wulst, is involved in vision in pigeons. The TeO measurements included the entire laminated portion of the TeO and therefore the tractus opticus and stratum opticum were not included. This is in agreement with previously published measurements of TeO volume (Boire 1989; Ebinger 1995; Iwaniuk et al. 2005).

In addition to measurements that we made ourselves, data for another 28 species were obtained from the literature (Ebinger and Lohmeier 1984; Boire 1989; Rehkemper et al. 1991; Alma and Bee de Speri 1992; Carezzano and Bee de Speri 1995; Ebinger 1995; Fernandez et al. 1997; Table 1). These studies used the same cytoarchitectonic criteria to define the boundaries of both Wulst and TeO as we did (see also Iwaniuk and Wyllie 2006).

### Eye size

The relative size of the Wulst and TeO might not only reflect the orientation of the orbits and binocularity, but also the relative size of the eyes themselves. By increasing the size of the eye, the focal length increases and the image is spread over more photoreceptors (Land and Nilsson 1993; Land and Nilsson 2002). If the number of photoreceptors determines the relative size of visual regions in the brain, then it is possible that eye size and brain region size will be correlated. In fact, relative eye size is correlated with relative brain size in birds (Garamszegi et al. 2002) and mammals (Burton 2006), which suggests that greater visual input (i.e., larger eyes) imposes greater processing demands on the brain. Some of this change in brain size could be because of enlargement of the Wulst and/or TeO, which comprise 1.6–26.8 and 2–11% of total brain volume, respectively (Iwaniuk and Hurley 2005). Thus, it is also

Second, there is a strong relationship between axial length and focal length (Murphy and Howland 1987). The focal length determines the size of the image on retina and is therefore related to the amount of visual information being received. Thus, if relative Wulst and/or TeO volume reflects visual input, then there should be a significant correlation between axial length and brain region volume. Eye measurements followed that are outlined in Ritland et al. (2004). Briefly, the axial length of the eye was measured to the nearest 0.01 mm with calipers from the center of the cornea to the posterior-most portion of the sclera directly opposite the cornea, slightly lateral to the exit point of the optic nerve.

To examine the relative size of the Wulst, we compared Wulst volume to brain volume and telencephalic volume. For both of these variables, we measured the volumes directly from the specimens. Brain volume was obtained by dividing the mass of the brain by the density of brain tissue (1.036 g/ml, Ebinger 1995; Iwaniuk and Nelson 2001, 2002). For the purposes of allometric analysis, we subtracted Wulst volume from both brain and telencephalon volumes and subtracted TeO volume from brain volume in order to effectively remove scaling effects (Deacon 1990; Iwaniuk et al. 2005). Although we made these corrections, we hereafter refer to these scaling variables as brain and telencephalon volumes.

We used both multiple regression analyses and residual analyses to test for significant relationship between relative Wulst or TeO volume and orbit orientation and eye size. Prior to all analyses, the data was log-transformed to create a linear relationship between allometrically related variables and to achieve a normal distribution. The multiple regression models used brain volume or telencephalon volume, orbit orientation (or axial length) and their interaction as effects of Wulst or TeO volume. Where the interaction effect was not significant, it was removed and the regression performed using least-squares linear regressions. For Wulst volume, we also examine the relationship with telencephalon volume,

which was expressed as total telencephalon volume minus Wulst volume (Iwaniuk and Wylie 2006). Where significant allometric relationships were present, we used the residuals from the regression lines as estimates of relative brain region volume and eye size. Due to a relatively small sample size, comparisons of binocular visual field and relative Wulst/TeO volume were restricted to analyses of residuals.

Because interspecific comparisons can be confounded by phylogenetic relationships (Harvey and Pagel 1991), we repeated these analyses using independent contrasts, commonly used phylogenetically based comparative method. Independent contrasts were calculated using the PDAP:PDTree module of the Mesquite software package (Maddison and Maddiso 2006). A phylogenetic tree was constructed on the basis of the inter-ordinal relationships of Sibley and Ahlquist (1990). Additional resolution for some clades was provided by other sources (Christidis et al 1991; Kimball et al. 1999; Sheldon et al 2000). Given the debate surrounding relationships within the caprimulgiform birds (see May 2002; Livezey and Zusi 2007), we tested several alternative topologies. We present the results of only one of these trees (Sibley and Ahlquist 1990), but note that using alternative trees did not affect the significance of our results. Because we constructed the trees from multiple sources, we used an arbitrary branch length model where each branch of the phylogeny was equal to 1. Diagnostic tests of the contrasts indicated that this branch model adequately standardized the data (Garland et al 1992).

Results

Orbit orientation and binocular visual field

The mean orbit orientation, as measured by convergence among 59 species measured was 37.96°, but there was a considerable amount of variation ranging from 16° in the green-cheeked Conure (*Pyrrhura molinae*) to almost 90° in the Grey Potoo.

Orbit orientation was significantly correlated with the size of the binocular field ( $F = 19.08, df = 1, 10, P < 0.01, r^2 = 0.62, \text{Fig. 3}$ ). Excluding the four species that we had congener data for did not affect the significance of this relationship ( $F = 8.78, df = 1, 6, P = 0.03, r^2 = 0.53, \text{Fig. 3}$ ). Using congener data, this relationship was corroborated by independent contrasts analyses ( $F = 9.11, df = 1, 8, P = 0.01, r^2 = 0.50$ ). Excluding the four species for which we only had congener data did not, however, result in the significant relationship being maintained ( $F = 2.78, df = 1, 5, P = 0.15$ ). Because of these mixed results, we analyzed both orbit orientation and binocular field with respect to the relative Wulst and TeO volumes.

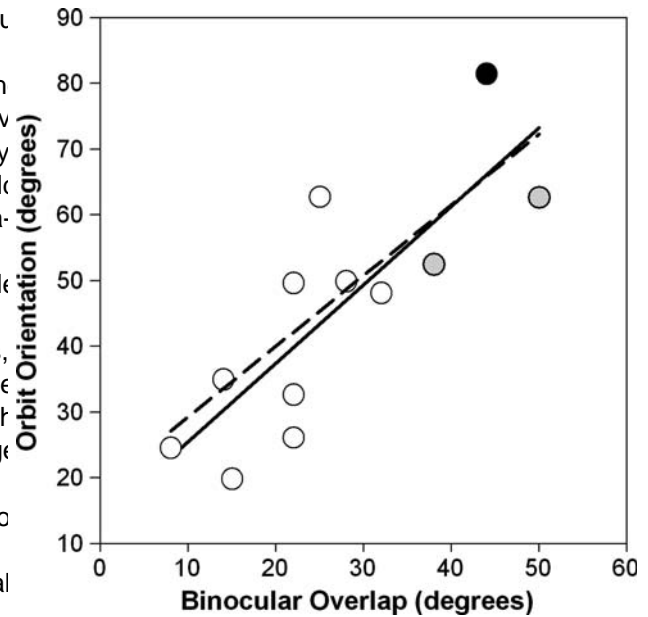


Fig. 3 A scatterplot of the amount of binocular visual field overlap (in degrees) plotted against the orbit orientation, as measured by degrees of convergence, for 12 species of birds. The black circle is the Barn Owl (*Tyto alba*), the gray circles are the Tawny Frogmouth (*Podargus strigoides*) and Oilbird (*Steatornis caripensis*) and the open circles represent all other species. The solid line indicates the least-squares linear regression line for all data and the dashed line indicates the least-squares linear regression line excluding those species for which we used congener data (see Materials and Methods)

Relative Wulst volume

Wulst volume (Fig. 4) scaled strongly against both brain ( $F = 164.63, df = 1, 58, P < 0.01, r^2 = 0.73$ ) and telencephalon volumes ( $F = 184.82, df = 1, 58, P < 0.01, r^2 = 0.76$ ). As expected from previous studies (Karten et al. 1973; Iwaniuk and Hurd 2005; Iwaniuk and Wylie 2006), the owls and several caprimulgiform birds [Tawny Frogmouth (*Podargus strigoides*), Feline Owllet-nightjar (*Aegotheles insignis*) and Oilbird (*Steatornis caripensis*)] were well above the regression line. At the opposite end of the spectrum, the parrots (Order Psittaciformes) and shorebirds (Order Charadriiformes) had relatively small Wulst volumes.

Relative TeO volume

Relative TeO volume was significantly correlated with brain volume ( $F = 95.78, df = 1, 58, P < 0.01, \text{Fig. 5}$ ), but the strength of this correlation was lower ( $r = 0.62$ ) than that of the Wulst and brain volume (see above). Unlike the Wulst, the TeO was relatively small in the owls. It was also relatively small in the parrots. At the opposite end of the spectrum, the Greater Rheas (*Rhea americana*, Order Rheiformes), egrets and herons (Order Ciconiiformes) and gallinaceous

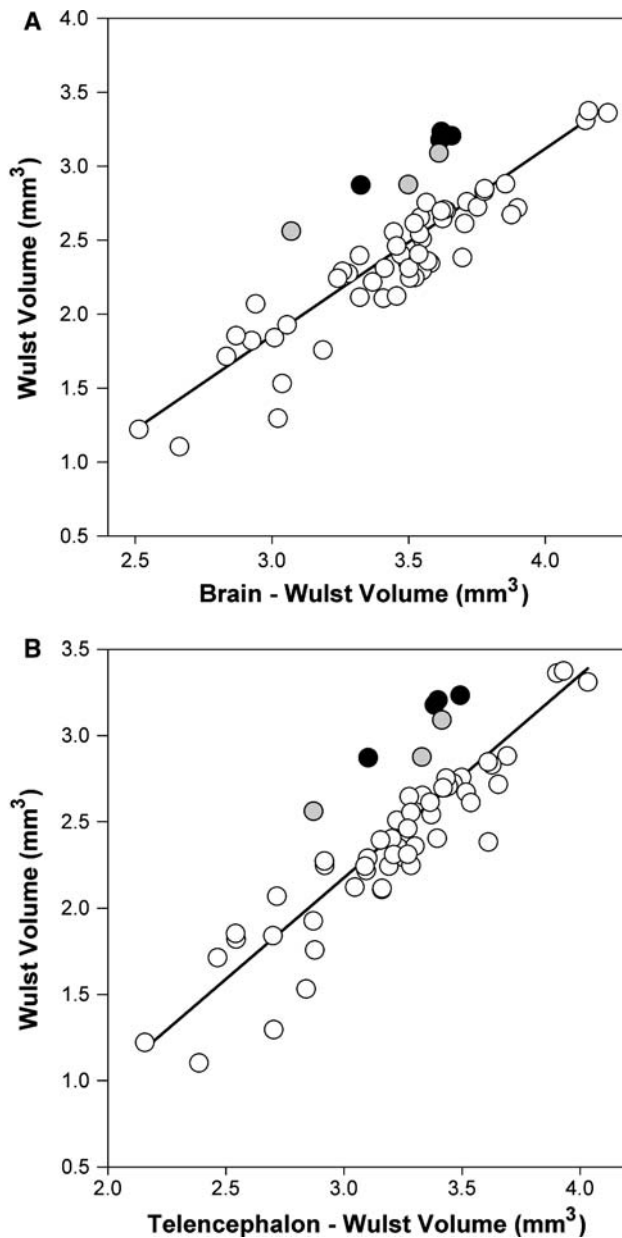


Fig. 4 Scatterplots of Wulst volume against brain minus Wulst volume (a) and Wulst volume (mm<sup>3</sup>) against telencephalon minus Wulst volume (b). For each plot, the solid line indicates the least-squares linear regression line. The black circles are the owls (Strigiformes), the gray circles are the Oilbird (*Steatornis caripensis*), Feline Owllet-nightjar (*Aegotheles insignis*) and the Tawny Frogmouth (*Podargus strigoides*) and the open circles are all other species sampled (see Table 6)

birds (Order Galliformes) all had relatively large TeO volumes.

#### Orbit orientation

Using brain volume and orbit orientation as independent variables, there was no significant interaction effect supported the multivariate models; relative to brain

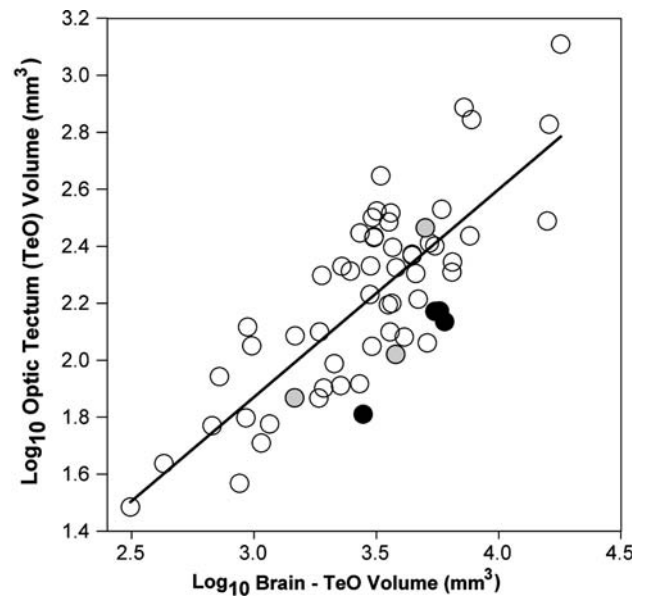


Fig. 5 A scatterplot of optic tectum (TeO) volume against brain minus TeO volume. The solid line indicates the least-squares linear regression line. The black circles are the owls (Strigiformes), the gray circles are the Oilbird (*Steatornis caripensis*), Feline Owllet-nightjar (*Aegotheles insignis*) and the Tawny Frogmouth (*Podargus strigoides*) and the open circles are all other species sampled (see Table 6)

( $F = 0.45, df = 1, 55, P = 0.50$ ), but there were significant effects of both brain volume ( $F = 220.57, df = 1, 56, P < 0.01$ ) and orbit orientation ( $F = 10.03, df = 1, 56, P < 0.01$ ) on Wulst volume. This pattern was identical in a multiple regression of telencephalic volume and orbit orientation on Wulst volume. No significant interaction effect was detected ( $F = 1.13, df = 1, 55, P = 0.29$ ), but there were significant effects of both telencephalic volume ( $F = 305.81, df = 1, 56, P < 0.01$ ) and orbit orientation ( $F = 23.35, df = 1, 56, P < 0.01$ ) on Wulst volume. Analyses of residuals provided very similar results; orbit orientation was significantly correlated with Wulst volume relative to both whole brain (Fig. 6a) and telencephalic (Fig. 6b) volumes.

Independent contrasts analyses largely corroborated these findings. Using brain volume as the scaling variable in a multiple regression, there was not a significant interaction effect ( $F = 0.07, df = 1, 52, P = 0.79$ ) or an orbit orientation effect ( $F = 2.47, df = 1, 53, P = 0.12$ ), but there was a significant effect of brain volume ( $F = 266.19, df = 1, 53, P < 0.01$ ) on Wulst volume. When we used telencephalon volume as a scaling variable, there was also no significant interaction effect ( $F = 0.75, df = 1, 52, P = 0.39$ ), but there were significant effects of both telencephalon volume ( $F = 310.67, df = 1, 53, P < 0.01$ ) and orbit orientation ( $F = 4.89, df = 1, 53, P = 0.03$ ) on Wulst

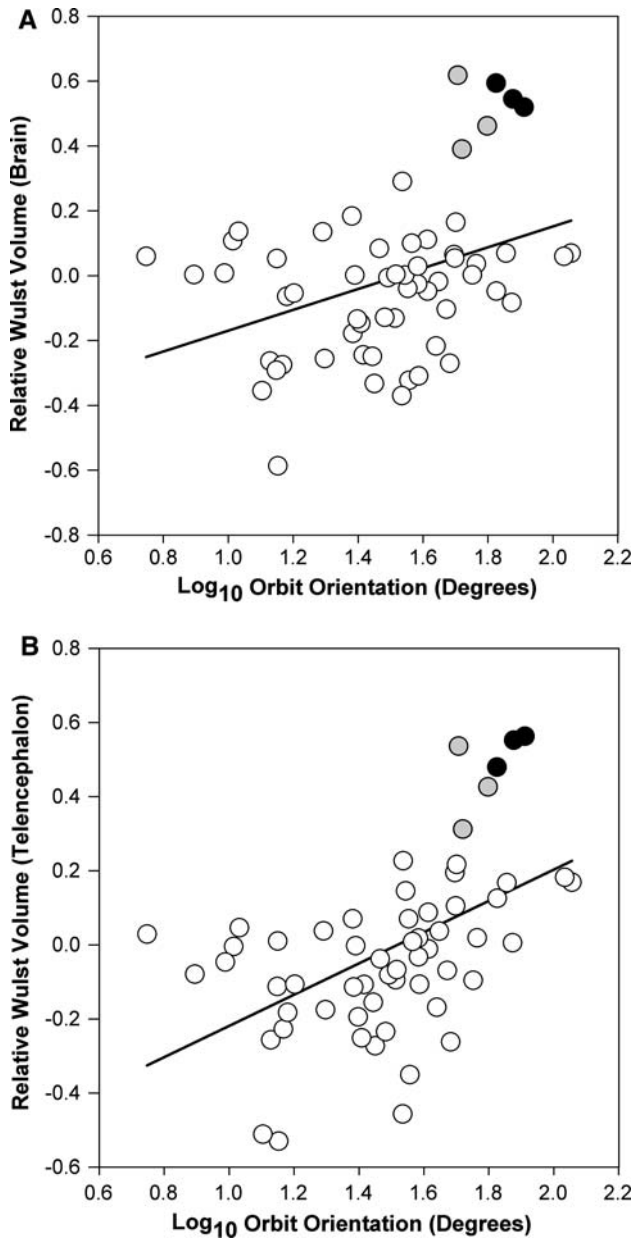


Fig. 6 Scatterplots of Wulst volume relative to brain volume (a) and forebrain volume (b) plotted against orbit orientation. Relative Wulst volumes are residuals derived from the least-squares linear regressions shown in Fig. 3. Wulst volumes were significantly correlated with orbit orientation when both brain volume ( $F = 9.26$ ,  $df = 1, 57$ ,  $P < 0.01$ ,  $r^2 = 0.12$ ) and telencephalic volume ( $F = 20.29$ ,  $df = 1, 57$ ,  $P < 0.01$ ,  $r^2 = 0.25$ ) were used as scaling variables. Solid lines indicate the least-squares linear regression lines. Black circles are the owls (*Strigiformes*), the gray circles are the Oilbird (*Steatornis caripensis*), the gray circle is the Feline Owlet-nightjar (*Aegotheles insignis*) and the gray circle is the Tawny Frogmouth (*Podargus strigoides*) and the open circles are all other species sampled (see Table 1)

volume, Wulst volume was not significantly correlated with orbit orientation ( $F = 0.18$ ,  $df = 1, 56$ ,  $P = 0.67$ ), but relative to telencephalon volume, Wulst volume was significantly correlated with orbital orientation ( $F = 12.01$ ,

$df = 1, 56$ ,  $P < 0.01$ ,  $r^2 = 0.14$ ). Thus, the size of the Wulst relative to the telencephalon is significantly correlated with orbit orientation.

Using brain volume and orbit orientation as independent variables, there was no significant interaction effect ( $F = 1.27$ ,  $df = 1, 56$ ,  $P = 0.27$ ) on TeO volume. The effect of orbit orientation was also not significant ( $F = 0.02$ ,  $df = 1, 57$ ,  $P = 0.88$ ), but a significant effect of brain volume was detected ( $F = 89.41$ ,  $df = 1, 57$ ,  $P < 0.01$ ). Again, analysis of TeO residuals (derived from Fig. 5) and orbit orientation yielded no significant relationship (Fig. 7a).

This was also true of the independent contrasts analyses; there was no significant interaction effect ( $F = 0.01$ ,  $df = 1, 52$ ,  $P = 0.93$ ) and no significant effect of orbit orientation ( $F = 0.05$ ,  $df = 1, 53$ ,  $P = 0.82$ ) on TeO volume. The significant relationship between brain and TeO volumes did, however, remain ( $F = 104.81$ ,  $df = 1, 53$ ,  $P < 0.01$ ). Similarly, analysis of independent contrasts of relative TeO volume and orbit orientation yielded no significant relationship ( $F = 0.98$ ,  $df = 1, 56$ ,  $P = 0.90$ ). Thus, there is no significant relationship between relative TeO volume and orbit orientation.

#### Binocular visual field

When we considered the species in which we had data from congeners, binocular visual field was significantly correlated with Wulst volume relative to both brain volume (Fig. 8a) and telencephalic volume (Fig. 8b). This was partially corroborated by independent contrasts analysis of the residuals; Wulst relative to brain volume was significantly correlated with binocular visual field ( $F = 4.95$ ,  $df = 1, 9$ ,  $P = 0.048$ ,  $r^2 = 0.31$ ), but Wulst relative to telencephalon volume was not ( $F = 1.84$ ,  $df = 1, 9$ ,  $P = 0.20$ ). Excluding the congener data yielded similar results. When species were analyzed as independent data points, a significant relationship was present (brain:  $F = 9.46$ ,  $df = 1, 7$ ,  $P = 0.02$ ; telencephalon:  $F = 7.20$ ,  $df = 1, 7$ ,  $P = 0.03$ ), but this disappeared with the application of independent contrasts (both  $P > 0.10$ ). Thus, we have mixed evidence that a relatively larger Wulst is correlated with broader binocular visual fields.

Analyses of binocular visual field and relative TeO volume yielded very similar results to that of orbit orientation, regardless of whether we included or excluded species for which we only had congener data. Although there was an apparent negative relationship between relative TeO volume and binocular visual field, this was not significant (Fig. 7b). Similarly, independent contrasts analysis yielded no significant relationship between

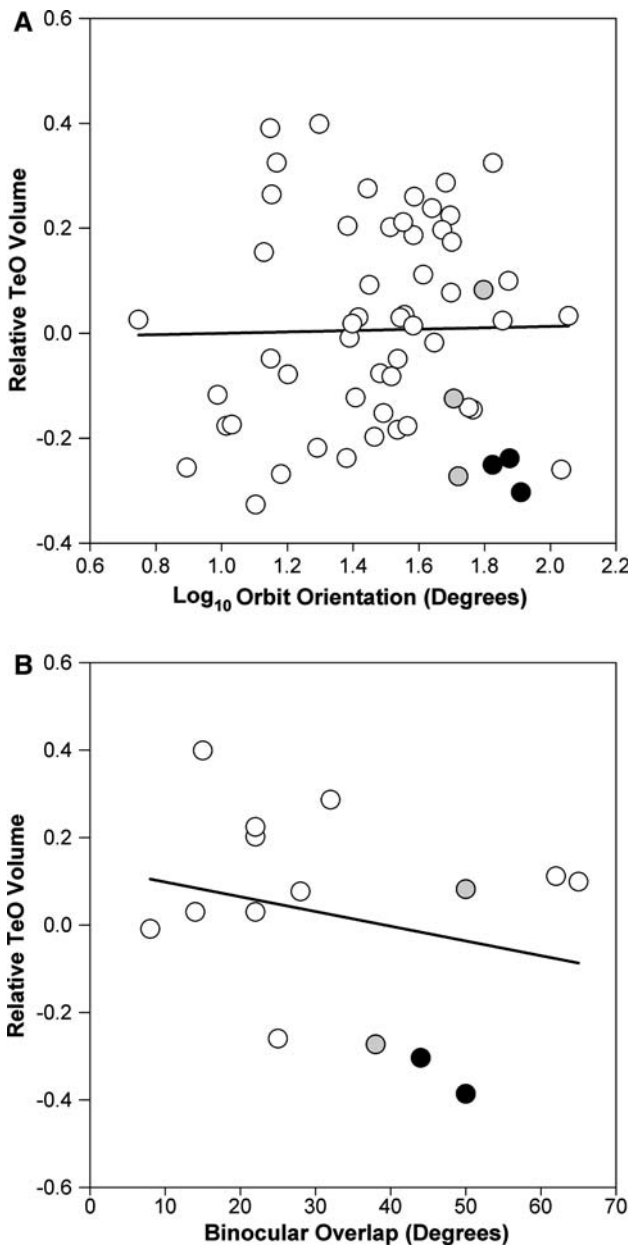


Fig. 7 A scatterplot of optic tectum (TeO) volume relative to brain volume plotted against orbital convergence; and B binocular visual field. Relative Wulst volumes are residuals derived from the least-squares linear regressions. TeO volumes were not significantly correlated with either orbital convergence ( $F = 0.02$ ,  $df = 1, 57$ ,  $P = 0.88$ ) or binocular visual field ( $F = 3.88$ ,  $df = 1, 11$ ,  $P = 0.07$ ). The solid lines indicate the least-squares linear regression lines. The black circles are the owls (Strigiformes), the gray circles are the Oilbird (*Steatornis caripensis*), the Feline Owlet-nightjar (*Aegotheles insignis*) and the Tawny Frogmouth (*Podargus strigoides*) and the open circles are all other species sampled (see Table)

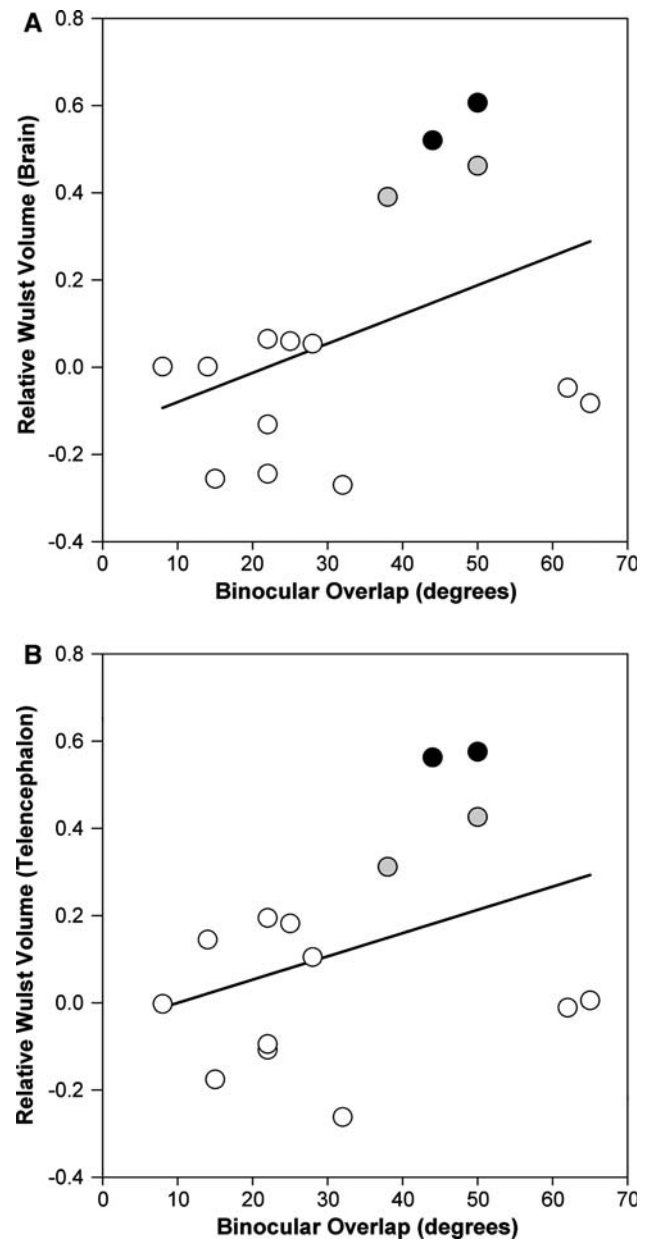


Fig. 8 Scatterplots of Wulst volume relative to brain volume (a) and telencephalon volume (b) plotted against binocular visual field. Relative Wulst volumes are residuals derived from the least-squares linear regressions. Wulst volumes were significantly correlated with the breadth of the binocular visual field when both brain volume ( $F = 17.91$ ,  $df = 1, 11$ ,  $P < 0.01$ ,  $r^2 = 0.58$ ) and telencephalic volumes ( $F = 12.11$ ,  $df = 1, 11$ ,  $P = 0.01$ ,  $r^2 = 0.48$ ) were used as scaling variables. The solid lines indicate the least-squares linear regression lines. The black circles are the owls (Strigiformes), the gray circles are the Oilbird (*Steatornis caripensis*) and the Tawny Frogmouth (*Podargus strigoides*) and the open circles are all other species sampled (see Table)

relative TeO volume and binocular visual field ( $F = 2.78$ ,  $df = 1, 8$ ,  $P = 0.13$ ; congener data excluded:  $F = 0.53$ ,  $df = 1, 6$ ,  $P = 0.49$ ). Thus, there is no significant relationship between relative TeO volume and binocularity.

Eye size  
The axial length of the eye was not available for all species in our study, but for the 44 species that we did have data,

axial length was significantly correlated with all three scaling variables: brain-Wulst volume ( $F = 28.53, df = 1, 42, P < 0.01, r^2 = 0.39$ ), telencephalon-Wulst volume ( $F = 16.57, df = 1, 42, P < 0.01, r^2 = 0.27$ ) and brain-TeO volume ( $F = 30.54, df = 1, 42, P < 0.01, r^2 = 0.41$ ). Residuals from these linear regressions were subsequently used as estimates of relative axial length of the eye. Within our sample, the Grey Potoo had the longest relative axial length, whereas the Green-cheeked Conure (*Pyrrhura molinae*) had the shortest relative axial length.

When we included axial length in a multiple regression model along with the scaling variables (brain and telencephalon volumes), we detected no significant interaction effects (brain:  $F = 1.13, df = 1, 40, P = 0.29$ ; telencephalon:  $F = 0.47, df = 1, 40, P = 0.50$ ) on Wulst volume. Relative to brain volume, there was no significant effect of axial length ( $F = 1.57, df = 1, 41, P = 0.22$ ) on Wulst volume, but there was a significant effect of axial length ( $F = 6.60, df = 1, 41, P = 0.01$ ) on Wulst volume relative to the telencephalon. In this latter model, axial length slightly increased the amount of variation explained by telencephalon alone ( $F = 2.77, df = 1, 41, P = 0.11, r^2 = 0.73$ ). To further clarify the relationship between axial length and Wulst volume, residual analyses were performed in a similar fashion to that provided for orbit orientation. Again, relative to brain volume, there was no significant relationship between Wulst volume and axial length ( $F = 1.61, df = 1, 42, P = 0.21$ , Fig. 9a). Relative to telencephalon volume, a significant positive relationship was detected ( $F = 6.75, df = 1, 42, P = 0.01, r^2 = 0.12$ ).

Independent contrasts analyses failed to detect any significant relationships between relative Wulst volume and axial length of the eye, regardless of whether a multiple regression model or residual analysis was used (all  $P > 0.13$ ). Residual analyses did not yield a significant relationship between axial length and relative Wulst volume, regardless of whether brain ( $F = 0.15, df = 1, 38, P = 0.72$ ) or telencephalon volume ( $F = 0.30, df = 1, 38, P = 0.61$ ) was used as a scaling variable.

Finally, analyses of TeO volume and axial length of the eye also failed to detect any significant effects. Using species as independent data points, a multiple regression model failed to find a significant interaction effect ( $F = 1.84, df = 1, 40, P = 0.18$ ), but did detect a significant effect of axial length ( $F = 4.54, df = 1, 41, P = 0.04$ ) on TeO volume. Residual analysis (Fig. 9c) corroborated this finding ( $F = 4.64, df = 1, 42, P = 0.04, r^2 = 0.08$ ). A multiple regression of the independent contrasts failed to detect any significant effect of axial length on TeO volume (interaction:  $F = 0.51, df = 1, 37, P = 0.48$ ; axial length:  $F = 1.12, df = 1, 38, P = 0.30$ ). An analysis of the independent contrasts of the residuals also failed to find a significant effect of axial length on TeO volume ( $F = 3.61, df = 1, 38, P = 0.07$ ). Thus, relative TeO

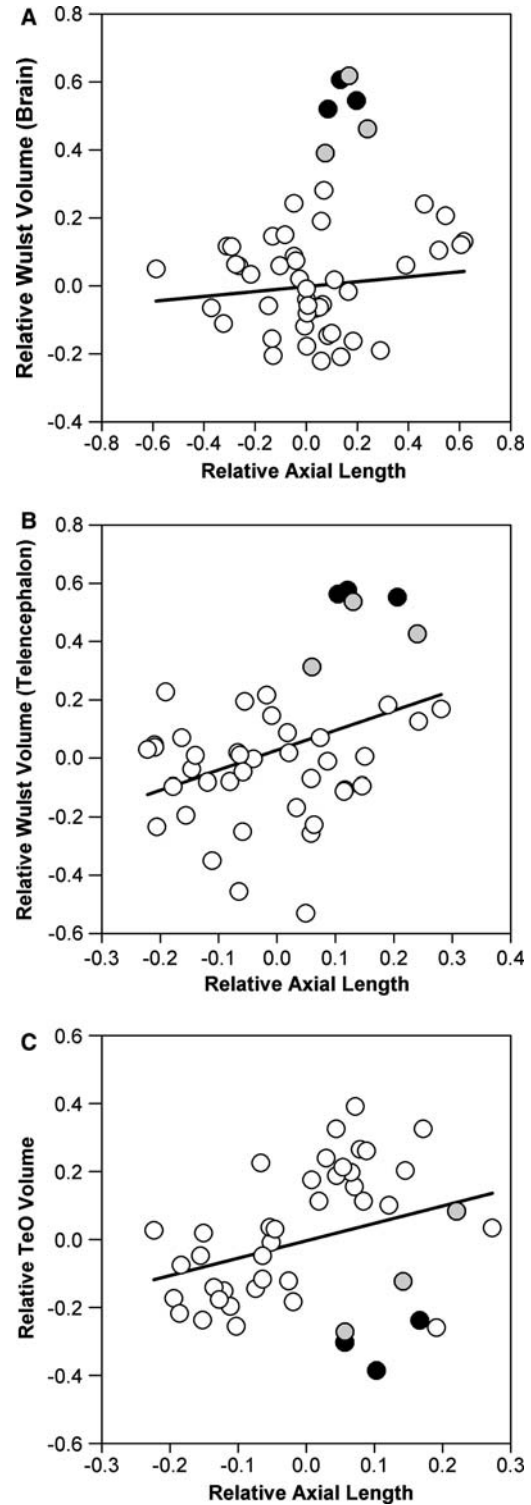


Fig. 9 Scatterplots of Wulst volume relative to brain volume (a), (Wulst volume relative to telencephalon volume) (b) and TeO volume relative to brain volume (c) plotted against relative axial length of the eye. The solid lines indicate the least-squares linear regression lines. The black circles are the owls (*Strigiformes*), the gray circles are the Oilbird (*Steatornis caripensis*), the white circles are the Feline Owllet-nightjar (*Megothiles insignis*) and the Tawny Frogmouth (*Podargus strigoides*) and the open circles are all other species sampled (see Table 1)

volume is not significantly correlated with relative axial binocular visual field, there are a number of factors that may be confounding this relationship, as discussed previously (see Introduction).

## Discussion

### Organization of the Wulst and optic tectum

Overall, our analyses indicate that orbit orientation is significantly correlated with relative Wulst volume, but not with relative TeO volume. In addition, a relatively larger Wulst volume is associated with a larger binocular visual field, which parallels similar findings in mammals (Barton 2004), but this relationship was not consistent across all of our analyses. Lastly, neither Wulst nor TeO reflect not only visual, but also somatosensory and motor volume were significantly associated with axial length of processing requirements. In some species, the border between visual and somato-motor Wulst can be defined by a sulcus (Manger et al. 2002), but possibly binocularly, our interpretation of these results is certainly not true of all birds and it is difficult to distinguish in coronally sectioned tissue. The inclusion of non-visual parts of the Wulst in our measurements could therefore weaken the strength of the relationships reported herein and at least partially explain why the correlations we

The correlation between relative Wulst volume and orbit orientation parallels a similar pattern between relative V1 and orbital convergence in primates (Barton 2004) and since the Wulst is a homolog of V1 (Medina and Reiner 2000; Reiner et al. 2005), this relationship is not entirely unexpected. As mentioned previously, the Wulst is the only forebrain region known to possess binocular disparity sensitive neurons that enable stereopsis (Pettigrew 1978, 1979). The extent to which the presence of binocular disparity sensitive neurons mirrors differences in relative Wulst volume, orbit orientation and width of the binocular visual field is mixed. Owls have a much broader area of horizontal binocular overlap (44–50°) (Martin 1984; Pettigrew and Konishi 1984; Wylie et al. 1994) and a relatively larger Wulst volume (Iwaniuk and Hurry 2005; Iwaniuk and Wylie 2006) than other birds (horizontal binocular overlap mean = 20°) (data from Martin and Katzir 1999). Moreover, the majority of HA neurons in owls are binocular disparity sensitive (Pettigrew 1978, 1979). Raptors also have far more binocular than monocular neurons in the visual Wulst (Pettigrew 1978), but their Wulst is relatively small and the binocular field occupies a much smaller portion of the entire visual field (Wallman and Pettigrew 1985; Martin and Katzir 1999). Finally, the Oilbird lacks binocular disparity sensitive neurons (Pettigrew and Konishi 1984), but has a moderately enlarged Wulst (Iwaniuk and Wylie 2006), more frontally placed eyes and a relatively large amount of binocular overlap in its visual field (Martin et al. 2004a, b). Although it is tempting to conclude that Wulst enlargement is correlated with orbit orientation and possibly the size of the

detected were lower than that in mammals (Barton 2004). A similar argument can be used to explain the lack of a significant correlation between orbit orientation and relative TeO volume. TeO, although primarily visual, also receives input from auditory nuclei and plays a key role in auditory and visual stimulus localization (Cottrell 1976; Knudsen 1982, 1984; Brainard and Knudsen 1995; Lewald and Dorscheidt 1998; Knudsen 2002). Thus, the inclusion of other visual and non-visual processing in the TeO could also confound any possible correlation between orbit orientation and TeO volume. Moreover, the Wulst may be subserving the binocular field in owls and caprimulgidiforms, but not in more laterally eyed species, such as pigeons (Gunterken and Hahman 1999).

the Oilbird is a curious exception. As noted previously (see Eye size above and Iwaniuk and Wylie 2006), the Oilbird has a significantly enlarged Wulst, but no disparity sensitive neurons (Pettigrew and Konishi 1984) and low spatial resolution based on their retinal morphology (Martin et al. 2004). Given the bizarre life history of this species, a variety of factors could be due to a number of factors. For example, axial length might not be able to determine why the Oilbird would require an enlarged Wulst based on its behaviour or ecology. Given that Oilbird nestlings develop in almost complete darkness (Wessels 1975) and this variation appears to be independent of eye size (e.g., McNeil et al. 2005). Given that visual input is dependent upon the number of photoreceptors, a more appropriate measure of eye size might be total photoreceptor density. Given the high density of photoreceptors in the Oilbird retina (Martin et al. 2004b), this, however, supposes that this could also explain why the Oilbird has an enlarged Wulst. Other measures that might show a significant relationship with relative Wulst or TeO volumes are ganglion cell numbers or optic nerve diameter, both of which also reflect the amount of incoming visual information. To our knowledge, there are insufficient data on retinal morphology among birds to test these predictions adequately at this time. Preliminary data collected by the authors (ANI, MGH) suggest that optic nerve diameter is not, however, correlated with relative Wulst volume.

## Eye movements

As previously mentioned, orbit orientation is not the only visual field; eye movements can also alter the configuration of the binocular field. This is especially true for birds as whole because medio-lateral eye movements vary greatly in amplitude among species and indicate that orbit orientation could potentially be used as an estimate of the binocular visual field (at least along the horizontal axis) in birds. These conclusions have important implications for reconstructing the sensory ecology and behaviour of fossil birds and non-avian reptiles (e.g., Stevens 2006). It may be possible to not only estimate the binocular visual field from skulls, but also the relative size of the Wulst from endocasts and ultimately stereoscopic abilities.

In contrast, the eyes of owls are capable of some movement (Steinbach and Money 1973; Steinbach et al. 1974), but are relatively static compared to some of the other species mentioned above. This diversity of eye movements among birds and the contribution of these movements to the shape of the visual field likely weaken the relationships between orbit orientation, the binocular visual field and relative Wulst volume. This diversity of eye movements in birds could also partially explain the weaker relationships reported herein compared to that of mammals (Bart 2004).

**Acknowledgments** We wish to thank Healesville Sanctuary, Springvale Veterinary Clinic, Bishop Museum, National Museum of Natural History (Washington, DC) and American Museum of Natural History for providing us with access to specimens. Funding for this study was provided to ANI from the Alberta Ingenuity Fund and the Natural Sciences and Engineering Research Council of Canada (NSERC), to MIH and CPH from the Jurassic Foundation and to DRWW from NSERC and Canada Research Chairs Program. All of the research reported herein was performed in accordance with the "Principles of animal care", publication No. 86D23, revised 1985 of the National Institute of Health and with the Canadian Council for Animal Care regulations.

## References

- Alma SB, Bee de Speroni N (1992) Indices cerebrales y composicion cuantitativa encefalica de *Aethene cucularia* y *Tyto alba* (Strigiformes: Strigidae y Tytonidae). *Facenas* (Argentina) 9:19–37
- Barton RA (2004) Binocularity and brain evolution in primates. *Proc Nat Acad Sci USA* 101:10113–10115
- Barton RA, Harvey PH (2000) Mosaic evolution of brain structure in mammals. *Nature* 405:1055–1058
- Beyer WH (1979) CRC standard mathematical tables, 25th edn. CRC Press, Boca Raton
- Boire D (1989) Comparaison quantitative de l'encephale de ses grades subdivisions et de relais visuels, trijumeaux et acoustiques chez 28 especes. PhD Thesis, Universite de Montreal, Montreal
- Brainard MS, Knudsen EI (1995) Dynamics of visually guided auditory plasticity in the optic tectum of the barn owl. *J Neurophysiol* 73:595–614
- Burton RF (2006) A new look at the scaling of size in mammalian eyes. *J Zool* 269:225–232
- Carezzano FJ, Bee de Speroni N (1995) Composicion volumetrica encefalica e indices cerebrales en tres aves de ambiente acuatico (Ardeidae, Podicipedidae, Rallidae). *Facenas* 11:75–83
- Cartmill M (1970) The orbits of arboreal mammals: a reassessment of the arboreal theory of primate evolution. Unpublished PhD dissertation, University of Chicago, Chicago
- Christidis L, Schodde R, Shaw DD, Maynes SF (1991) Relationships among the Australo-Papuan parrots, lorikeets and cockatoos (Aves: Psittaciformes). *Condor* 93:302–317
- Cotter JR (1976) Visual and nonvisual units recorded from the optic tectum of *Gallus domesticus*. *Brain Behav Evol* 13:1–21
- Deacon TW (1990) Fallacies of progression in theories of brain-size evolution. *Int J Primatol* 11:193–236
- Deng C, Wang B (1993) Convergence of somatic and visual afferent impulses in the Wulst of pigeon. *Exp Brain Res* 96:287–290
- Ebinger P (1995) Domestication and plasticity of brain organization in mallards *Anas platyrhynchos*. *Brain Behav Evol* 45:286–300
- Ebinger P, Lamer R (1984) Comparative quantitative investigations on brains of rock doves, domestic and urban pigeons (*Columba livia*). *Zool Syst Evolut-forsch* 22:136–145
- Fernandez P, Carezzano F, Bee de Speroni N (1997) Indices cuantitativo encefalico e indices cerebrales de *Aratinga acuticaudata* *Myopsitta monachula* de Argentina (Aves: Psittacidae). *Rev Chil Hist Nat* 70:269–275
- Fite KV, Rosenfeld-Wessels S (1975) A comparative study of deep avian foveas. *Brain Behav Evol* 12:97–115
- Funke K (1989) Somatosensory areas in the telencephalon of the pigeon. I. Response characteristics. *Exp Brain Res* 76:603–619
- Garland T Jr, Harvey PH, Ives AR (1992) Procedures for the analysis of comparative data using phylogenetically independent contrasts. *Syst Biol* 41:18–32
- Garamszegi LZ, Moller AP, Erritzoe J (2002) Coevolving avian eye size and brain size in relation to prey capture and nocturnality. *Proc R Soc Lond B* 269:961–967
- Güntürkün O, Hahmann U (1999) Functional subdivisions of the ascending visual pathways in the pigeon. *Behav Brain Res* 98:193–201
- Hall MI, Ross CF (2007) Eye shape and activity pattern in birds. *J Zool* 271:437–444
- Harvey PH, Pagel MD (1991) The comparative method in evolutionary biology. Oxford University Press, Oxford
- Heesy CP (2003) The evolution of orbit orientation in mammals and the function of the primate postorbital bar. PhD Dissertation, Stony Brook University, Stony Brook
- Heesy CP (2004) On the relationship between orbit orientation and binocular visual field overlap in mammals. *Anat Rec* 281A:1104–1110
- Howland HC, Merola S, Basarab JR (2004) The allometry and scaling of the size of vertebrate eyes. *Vis Res* 44:2043–2065
- Husband S, Shimizu T (2001) Evolution of the avian visual system. In: Cook RG (ed) *Avian visual cognition*. <http://www.pigeon.psy.tufts.edu/avc/husband/>
- Iwaniuk AN, Hurd PL (2005) A multivariate analysis of cerebrotypes in birds. *Brain Behav Evol* 65:215–230
- Iwaniuk AN, Nelson JE (2002) Can endocranial volume be used as an estimate of brain size in birds? *Can J Zool* 80:16–23
- Iwaniuk AN, Nelson JE (2001) A comparative analysis of relative brain size in waterfowl (Anseriformes). *Brain Behav Evol* 57:87–97
- Iwaniuk AN, Wylie DRW (2006) The evolution of stereopsis and the Wulst in caprimulgiform birds: a comparative analysis. *J Comp Physiol A* 192:1313–1326
- Iwaniuk AN, Dean KM, Nelson JE (2004) A mosaic pattern characterizes the evolution of the avian brain. *Proc R Soc Lond B* 271:S148–S151
- Iwaniuk AN, Dean KM, Nelson JE (2005) Interspecific allometry of the brain and brain regions in parrots (Psittaciformes): comparisons with other birds and primates. *Brain Behav Evol* 65:40–59
- Karten HJ, Hodos W, Nauta WJH, Revzin AM (1973) Neural connections of the visual Wulst of the avian telencephalon: Experimental studies in the pigeon (*Columba livia*) and owl (*Speotyto cucularia*). *J Comp Neurol* 150:253–278
- Katzir G, Martin GR (1994) Visual fields in herons (Ardeidae): panoramic vision beneath the bill. *Naturwissenschaften* 81:182–184
- Katzir G, Martin GR (1998) Visual fields in the Black-crowned Night Heron *Nycticorax nycticorax*: nocturnality does not result in owl-like features. *Ibis* 140:157–162
- Kaye M, Mitchell DE, Cynader M (1981) Depth perception, eye alignment and cortical ocular dominance of dark-reared cats. *Brain Res* 254:37–53
- Kimball RT, Braun EL, Zwartjes PW, Crowe TM, Ligon JD (1999) A molecular phylogeny of the pheasants and partridges suggests that these lineages are not monophyletic. *Mol Phylogenet Evol* 11:38–54
- Knudsen EI (1982) Auditory and visual maps of space in the optic tectum of the owl. *J Neurosci* 2:1177–1194
- Knudsen EI (1984) Auditory properties of space-tuned units in owl's optic tectum. *J Neurophysiol* 52:709–723
- Knudsen EI (2002) Instructed learning in the auditory localization pathway of the barn owl. *Nature* 417:322–328
- Krutzfeldt NO, Wild JM (2005) Definition and novel connections of the entopallium in the pigeon (*Columba livia*). *J Comp Neurol* 490:40–56
- Land MF (1980) Optics and vision in invertebrates. In: Antrum H (ed) *Handbook of sensory physiology VII/6B*. Springer, Berlin, pp 471–592
- Land MF, Nilsson D-E (2002) *Animal eyes*. Oxford University Press, New York
- Lewald J, Dorrscheidt GJ (1998) Spatial-tuning properties of auditory neurons in the optic tectum of the pigeon. *Brain Res* 790:339–342
- Livezey BC, Zusi RL (2007) Higher-order phylogeny of modern birds (Theropoda, Aves: Neornithes) based on comparative anatomy. II. Analysis and discussion. *Zool J Linn Soc* 149:1–95
- Lockwood CA, Lynch JM, Kimbel WH (2002) Quantifying temporal bone morphology of great apes and humans: an approach using geometric morphometrics. *J Anat* 201:447–464
- Maddison WP, Maddison DR (2006) *Mesquite: a modular system for evolutionary analysis*. Version 1.1 <http://mesquiteproject.org>

- Manger PR, Elston GN, Pettigrew JD (2002) Multiple maps and activity-dependent representational plasticity in the anterior Wulst of the adult barn owl (*Tyto alba*). *Eur J Neurosci* 16:743–750
- Martin GR (1984) The visual fields of the tawny owl (*Nyctaleus alba*). *Vis Res* 24:1739–1751
- Martin GR (1986) Total panoramic vision in the mallard duck (*Anas platyrhynchos*). *Vis Res* 26:1303–1305
- Martin GR (1993) Producing the image. In: Zeigler HP, Bischof H-J (eds) *Vision, brain, and behavior in birds*. MIT, Cambridge, pp 5–24
- Martin GR (1994) Visual fields in woodcock (*Scolopax rusticola*, Scolopacidae; Charadriiformes). *J Comp Physiol A* 174:787–793
- Martin GR (1999) Optical structure and visual fields in birds: their relationship with foraging behaviour and ecology. In: Archer SN, Djamgoz MBA, Loew ER, Partridge JC, Vallerga S (eds) *Adaptive mechanisms in the ecology of vision*. Kluwer, Norwell, pp 485–508
- Martin GR, Coetzee HC (2004) Visual fields in hornbills: precision-grasping and sunshades. *Ibis* 146:18–26
- Martin GR, de Brooke ML (1991) The eye of a procellariiform seabird, the Manx shearwater (*Puffinus puffinus*): visual fields and optical structure. *Brain Behav Evol* 37:65–78
- Martin GR, Katzir G (1999) Visual fields in short-toed eagles, *Circus gallicus* (Accipitridae), and the function of binocularity in birds. *Brain Behav Evol* 53:55–66
- Martin GR, Rojas LM, Figueroa YMR, McNeil R (2004a) Binocular vision and nocturnal activity in oilbirds (*Steatornis caripensis*) and parakeets (*Nyctidromus albigollis*; Caprimulgiformes). *Orn Neotrop* 15:233–242
- Martin GR, Rojas LM, Ramirez Y, McNeil R (2004b) The eyes of oilbirds (*Steatornis caripensis*) pushing at the limits of sensitivity. *Naturwiss* 91:26–29
- Martin GR, Young SR (1984) The eye of the Humboldt penguin, *Spheniscus humboldti*: visual fields and schematic optics. *Proc R Soc Lond B* 223:197–222
- Martinoya C, LeHouezec J, Bloch S (1984) Pigeons' eyes converge during feeding: evidence for frontal binocular fixation in a lateral-eyed bird. *Neurosci Lett* 45:335–339
- Mayr G (2002) Osteological evidence for paraphyly of the avian order Caprimulgiformes (nightjars and allies). *J Ornithol* 143:82–97
- McFadden SA, Wild JM (1986) Binocular depth perception in the pigeon. *J Exp Anal Behav* 45:149–160
- McNeil R, McSween A, Lachapelle P (2005) Comparison of the retinal structure and function in four bird species as a function of the time they start singing in the morning. *Brain Behav Evol* 65:202–214
- Medina L, Reiner A (2000) Do birds possess homologues of mammalian primary visual, somatosensory and motor cortices? *Trends Neurosci* 23:1–12
- Miceli D, Gioanni H, Reppert J, Peyrichoux J (1979) The avian visual Wulst: I. An anatomical study of afferent and efferent pathways. II. An electrophysiological study of the functional properties of single neurons. In: Granda AM, Maxwell JH (eds) *Neural mechanisms of behavior in birds*. Plenum Press, New York, pp 223–354
- Murphy CJ, Howland HC (1987) The optics of comparative ophthalmology. *Vis Res* 27:599–607
- Nguyen AP, Spetch ML, Crowder NA, Winship IR, Hurd PL, Wylie DR (2004) A dissociation of motion and spatial-pattern vision in the avian telencephalon: implications for the evolution of visual streams. *J Neurosci* 24:4962–4970
- Pettigrew JD (1978) Comparison of the retinotopic organization of the visual wulst in nocturnal and diurnal raptors, with a note on the evolution of frontal vision. In: Cool SJ, Smith EL (eds) *Frontiers in visual science*. Springer, New York, pp 328–335
- Pettigrew JD (1979) Binocular visual processing in the owl's telencephalon. *Proc R Soc Lond, B* 204:435–454
- Pettigrew JD, Konishi M (1976a) Neurons selective for orientation and binocular disparity in the visual Wulst of the barn owl (*Tyto alba*). *Science* 193:675–678
- Pettigrew JD, Konishi M (1976b) Effect of monocular deprivation on binocular neurons in the owl's visual Wulst. *Nature* 264:753–754
- Pettigrew JD, Konishi M (1984) Some observations on the visual system of the oilbird, *Steatornis caripensis*. *Nat Geo Soc Res Rep* 16:439–450
- Proctor NS, Lynch PJ (1993) *Manual of ornithology: avian structure and function*. Yale University Press, New Haven
- Reep RL, Finlay BL, Darlington RB (2007) The limbic system in mammalian brain evolution. *Brain Behav Evol* 70:57–70
- Rehder G, Frahm HD, Zilles K (1991) Quantitative development of brain and brain structures in birds (Galliformes and Passeriformes) compared to that in mammals (insectivores and primates). *Brain Behav Evol* 37:125–143
- Reiner A, Yamamoto K, Karten HJ (2005) Organization and evolution of the avian forebrain. *Anat Rec A* 287:1080–1102
- Ritland S (1982) The allometry of the vertebrate eye. PhD Thesis, University of Chicago, Chicago
- Sheldon FH, Jones CE, McCracken KG (2000) Relative patterns and rates of evolution in heron nuclear and mitochondrial DNA. *Mol Biol Evol* 17:437–450
- Shimizu T, Karten HJ (1993) The avian visual system and the evolution of the neocortex. In: Zeigler HP, Bischof HJ (eds) *Vision, brain and behavior in birds*. MIT, Cambridge, pp 103–114
- Sibley CG, Ahlquist JE (1990) *Phylogeny and classification of birds*. Yale University Press, New Haven
- Steinbach MJ, Money KE (1973) Eye movements of the owl. *Vis Res* 13:889–891
- Steinbach MJ, Angus RG, Money KE (1974) Torsional eye movements of the owl. *Vis Res* 14:745–746
- Stevens KA (2006) Binocular vision in theropod dinosaurs. *J Vert Paleontol* 26:321–330
- Wallman J, Pettigrew JD (1985) Conjugate and disjunctive saccades in two avian species with contrasting oculomotor strategies. *J Neurosci* 5:1418–1428
- Whiting BA, Barton RA (2003) The evolution of the cortico-cerebellar complex in primates: anatomical connections predict patterns of correlated evolution. *J Hum Evol* 44:3–10
- Wild JM (1997) The avian somatosensory system: the pathway from wing to Wulst in a passerine (*Chloris chloris*). *Brain Res* 759:122–134
- Wild JM, Williams MN (2000) Rostral wulst in passerine birds. I. Origin, course, and terminations of an avian pyramidal tract. *J Comp Neurol* 416:429–450
- Wilson P (1980) The organization of the visual hyperstriatum in the domestic chick. II. Receptive field properties of single units. *Brain Res* 188:333–345
- Wylie DR, Frost BJ (1990) Binocular neurons in the nucleus of the basal optic root (nBOR) of the pigeon are selective for either translational or rotational visual flow. *Visual Neurosci* 5:489–495
- Wylie DR, Shaver SW, Frost BJ (1994) The visual response properties of neurons in the nucleus of the basal optic root of the northern saw-whet owl (*Aegolius acadicus*). *Brain Behav Evol* 43:15–25